

Enabling the rapid scale-up of concrete additive manufacturing

G. Finlayson, B. Hasday, A. Grobicki, T. Oeste, H. Simpson

Capstone Design Final Report

Department of Materials Science and Engineering

University of Maryland, College Park

INTRODUCTION

Motivation

One of the Grand Challenges given by the National Academy of Engineering is to restore and improve urban infrastructure.¹ Many aspects of public infrastructure are, or can be, made from concrete. These include bridges, dams, levees, roads, and sidewalks, as well as the buildings associated with power distribution and water and sewer systems. Making effective concrete mixtures for additive manufacturing could lower the cost of implementing these systems by bringing a new level of automation into the construction industry, in the same way that the assembly line and industrial robotics both brought incredible advances to manufacturing. The construction industry still heavily relies on manual work to complete projects, and these projects, such as office buildings and bridges, can cost millions of dollars. As such, there are far-reaching gains to be had in improving construction processes. Furthermore, there are many parties interested in lowering the costs of infrastructure, as well as the efficiency with which it can be put into place. Automated construction would benefit urban environments as much as it would also benefit disaster zones and impoverished areas, were infrastructure is too expensive to build or maintain.

The major bottleneck in the implementation of concrete additive manufacturing (AM) is a materials science problem: how can concrete be fluid enough to flow through a printer without clogging, viscous enough to hold its shape after printing, cure such that it bonds completely to the layers above and below it, all while maintain the mechanical properties needed for structural integrity? Many mechanical and chemical properties must be tuned in order for the component to be sound. The concrete must be extremely consistent, both in its fresh and cured properties, so that the structure itself has consistent properties that comply with building regulations. The porosity of the mix relates directly to its density, and this factor is important depending on whether the component will be critically loaded or not (some elements of the roofing will likely be designed to be lighter than the foundation and main walls). These problems are being addressed in current research, but a satisfactory solution has not yet been found.^{2,3} Studies have been performed on both the fresh and hardened properties on concrete, and these have included attempts to model the extrusion characteristics of fiber reinforced concrete mixtures.

Previous Work

While the practice of additive manufacturing with concrete is very recent, it is an active area of research. Three processes have arisen that allow for concrete to be deposited in three dimensions: Contour Crafting, d-shape, and Concrete Printing. Our work in this project is aimed at applications with Concrete Printing

and possibly Contour Crafting. Contour Crafting is a major step forward in concrete printing, which implements other robotic systems to assist in construction process and uses a trowel to smooth surfaces deposited surfaces. This research is headed by Dr. Behrokh Khoshnevis and is currently capable of manufacturing macro-scale structures. D-shape is a powder-deposition process whereby most any sand-like powder can be used to construct large structures. There are applications here for Lunar structures using Lunar dust. This process, while also capable of producing macro-scale structures, is not an extrusion process and so not relevant to this project. Finally, Concrete Printing offers finer resolution than contour crafting, and it uses a nozzle without a trowel to deposit single concrete filaments that can be built up into structures.⁴

More recent studies have been done into the material properties of concrete as they relate to additive manufacturing; both fresh and hardened properties must be accounted for in order to successfully print. The article “Rheology of semi-solid fresh cement pastes and mortars in orifice extrusion,” by Zhou et al. (2013) details an orifice extruder used to calculate the rheological properties of fresh concrete paste.⁵ It was found that the conventional methods of rheological testing were not applicable to printing concrete, which is significantly more viscous than pouring concrete. This paper lays the groundwork for our project, where we intend to use this new rheological testing instrument to yield material properties that can be used to further enable a simulation of the extrusion process.

Intellectual Merit And Impact

The primary purpose of this research is to develop a rheological model of concrete extrusion, which could be of use to all researchers currently working in this field. The second purpose is to determine if voids can be purposefully created in extruded parts through the use of entrained air as an admixture. This is a common practice for poured concrete to combat freeze-thaw damage, but the effects of entrained air in extruded concrete are not yet well defined. The final purpose of this research is to determine the rheological properties of the extruded concrete with entrained air. This can then be used to properly model the extrusion process. We believe that meeting any of these goals would benefit the scientific community.

The ability to extrude concrete with high strength allows for a large scalability of 3-D concrete printing. Architects and civil engineers want a way in which complex shapes can be created without building intricate molds. Construction firms would like to have faster turnaround when building houses or small structures, and because 3-D printing does not require human assistance, what could have taken weeks to complete can possibly be finished in as little as 48 hours.⁶ In an emergency situation, 3-D concrete printers could be taken to assist in relief efforts. The printer could be used to rebuild houses, clinics, schools and more. Again, the printer works without human assistance and can easily finish more rebuilding in less time, all while using a building material that is both incredibly abundant and cheap. For military applications, stronger fortified bases can be built in more remote or forward positions.

This research intends to model the nozzle flow characteristics to aid in scaling up current 3-D printing technologies. This research also intends to prove that extruded concrete can be made with entrained air, which is important for buildings in cold climates. To combat freeze thaw cycles, concrete is premixed with a surfactant to form air bubbles in the concrete as it cures. These air bubbles create voids that give expanding

water in cold weather a place to fill. The ability to build lasting, strong structures in numerous climates increases the versatility of a 3-D concrete printer.

Project Selection Process And Evolution

This project has evolved considerably since the beginning of the semester, when Tom Oeste selected the topic because of his interest in advanced manufacturing and construction technologies, including his own research at NIST involving human-robot collaborative systems. It was also thought that a project involving macro material properties would provide an interesting contrast against much of the research done by other Capstone groups. Initially, the goal was to create a rudimentary 3D printer that could deposit lines of concrete on top of each other and study the effects of concrete composition on interlayer bonding and hardened strength. This seemed to stray too far into mechanical engineering and exceed the scope of a one-semester design course. For the short list presentation, the project focus was narrowed to the extrusion process only, particularly on investigating the flow behavior of the concrete paste within an extruder. A simulation was also added at this stage, although it was unclear what simulation method would be used. By the proposal presentation, an elaborate testing scheme was developed to study the effects of air entraining admixture on the hardened properties of both poured and extruded concrete. A fractional factorial experiment was proposed to determine the parameter effects of several concrete constituents. As the semester progressed, it became clear that the design and prototype fabrication process would take longer than initially projected, and so less emphasis was placed on completing the fractional factorial experiment and mechanical testing, and more emphasis was placed on developing and validating the model. As it became clear that the machinist was having some difficulty completing the apparatus, and it would be some additional weeks until we had our prototype, we had to change project scope once again. While we were still interested in studying the effects of air entraining admixture (particularly air bubble size) on fresh concrete properties, our main concern was developing an effective model that complemented the extruder-rheometer. This was the final stage of our project, where we looked to develop a computational fluid dynamics model of the extrusion process based on material properties measured by the extruder apparatus, and we have found success in this effort.

EXPERIMENTAL METHOD

Technical Approach

The rheological data was obtained using an extrusion-based method developed by Zhou et al.⁵, where it is assumed that the concrete paste follows a generalized uniaxial-form of the Herschel-Bulkley relationship,

$$\sigma = \sigma_0 + k(\epsilon^{vp})^n$$

where σ is the uniaxial flow stress, σ_0 is the uniaxial yield flow stress, k is the uniaxial flow consistency and n is the uniaxial flow index. ϵ^{vp} is the equivalent viscoelastic strain rate.⁵ The authors translated this equation into terms of extrusion pressure and extruded flow velocity, and so it is possible to fit the three Herschel-Bulkley parameters to data taken from several extrusion tests with varying constant ram driving velocities. We attempted to use this technique to obtain the material parameters for our own, custom batches of concrete. Afterwards, these parameters can define the concrete material within our simulation, allowing a researcher to import the physical sample into their simulation.

The extruder was designed to interface with the Tinius Olsen Universal Testing Machine (UTS) in the Modern Engineering Materials Instructional Laboratory (MEMIL). The UTM powers the ram and records time, displacement, and force data. Before the extruder is assembled and bolted to the UTM, every part is cleaned with a damp cloth to remove dirt and any residual concrete. After cleaning, the bottom plate is bolted to the lower frame of the UTM, and the hopper is set in place. Cement, PVA fibers, retarder, plasticizer, surfactant, and fly ash are mixed dry in a plastic tub. Water is added to the dry mixture at a four-to-one ratio. A concrete mixer and electric drill are used to stir the fresh concrete until thoroughly mixed. The concrete is then stirred an extra 30 seconds or two minutes after the initial mixing to activate the surfactant and create two different sizes of entrained air bubbles. The hopper is then filled with fresh concrete until there is only room left for the height of the ram. The ram and top plate are set in place and secured to the rest of the apparatus. The UTM driving clamp is brought down to the height of the piston arm and secured to the apparatus. The driving speed is set to 0.1mm/s for the first minute of extrusion (meant to push out entrapped air and start concrete flow from the die), followed by a varied ram speeds ranging from 0.02mm/s to 0.6mm/s. As concrete is extruded, samples are collected and removed from the extrusion region. The ram is stopped as it approaches the static region inside the bottom of the hopper. This static region exists in the bottom region of the hopper surrounding the orifice where a slip system is setup and no flow occurs.

In addition to our physical experiments, we created a Computational Fluid Dynamics (CFD) model for our extrusion process. With this model, created using the ANSYS FLUENT program, we hoped to understand the rheological behavior of concrete and the additives comprising it. Specifically, we hoped that our model would accurately portray the distribution and size of sand aggregate and air bubbles in the concrete after extrusion. One model followed the Herschel-Bulkley model for non-Newtonian fluids, in which a fluid will behave as a rigid solid under low stress, before flowing at high stresses.⁷ While this may be an accurate model for the highly viscous cement fluid, it is beyond ANSYS FLUENT's capabilities to model both a Herschel-Bulkley fluid and a discrete particulate phase at the same time (another program, ANSYS POLYFLOW, has this capability; it was not available through the University's Virtual Computer Lab). Due to this programming limitation, we created a second model using a Discrete Phase Model (DPM) in FLUENT. In this case, the cement is modeled as a Newtonian fluid with two discrete particle phases: the sand (or other aggregate) and the air bubbles.

Facilities

Our group utilized the Modern Engineering Materials Instructional Laboratory (MEMIL) for all of our experiments. Originally, it was planned to use drying racks, as well as a freezer, to test and store samples. However, as the project progressed, our scope changed and we focused our testing and facility needs primarily on the ability to test the rheology of our fresh cement mixtures. The MEMIL lab had everything we needed; space to mix our concrete batches using a power drill (with an attached grout mixer), and the Tinius Olsen UTM, which powered our extrusion device and recorded data. We used tarps to cover up the UTM as well as the floor space where concrete mixtures were present. Dr. Robert Bonenberger was available both days that we worked in the MEMIL lab and helped us attach our extrusion machine to the UTM and use the software that ran it. We utilized the MEMIL lab for two days, eight hours each. Our use of the MEMIL lab was free, due to the status of our project as an academic requirement.

RESULTS

Simulation

The CFD models were based on fluid domains created from simplified CAD models of the extrusion device. The CAD models were simplified to contain only the hopper, the die surface, and a region for the extruded material to flow into. This simplification allows for less computational time for each calculation of the model. “Capping” the extruder model – that is, creating boundary surfaces covering the inlet and outlet of the extruder CAD model – created the fluid domain. A solid was then generated containing the region bounded by the extruder and the “caps.” The original extruder piece was then suppressed so that only the interior volume was meshed. At this point the CFD model was branched into two types – one following the Herschel-Bulkley model and another using a discrete particle method.

Herschel-Bulkley

The Herschel-Bulkley ANSYS FLUENT model calculates the behavior of a non-Newtonian fluid. The parameters used for the cement were taken from an additional paper by Zhou and his group.⁸

Yield Stress	σ_0	11.4 kPa
Flow Index	n	0.44
Viscosity	η	250 Pas
Consistency Index	κ	203.6 kPa

The cement flowed into the fluid domain at 1mm/s. Pressure measured on the orifice plane is show in **Figure 1**.

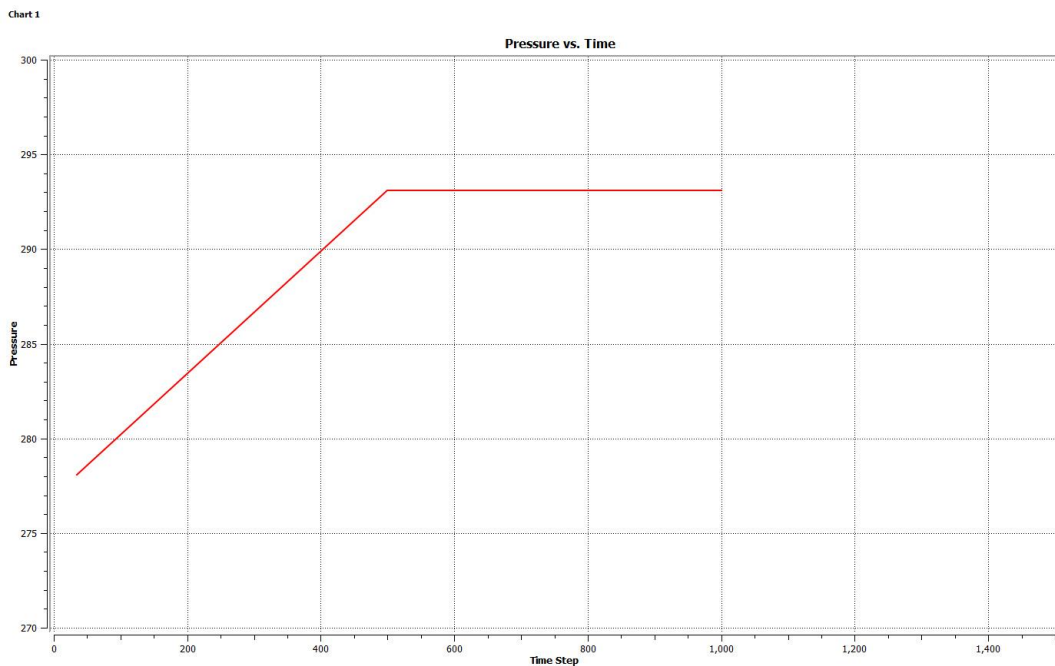


Figure 1. Pressure at the orifice plane in a FLUENT simulation of extrusion at a rate of 1 mm/s.

This generally agrees with the behavior found in our experimental data, which is discussed in detail in the Analysis of Results section.

Discrete Particle Method

In this model, the cement paste was regarded as a Newtonian fluid phase. Both the sand aggregate and the entrained air bubbles were modeled as discrete inert particle phases with average particle diameters of 500 μm and 1mm, respectively. Results using this model were of poor quality and did not accurately reflect our experimental data. We need more accurate material property measurements (e.g. cement viscosity, sand and air mass flow rates, particle size distribution) for this model to have potentially meaningful results.

Prototype Design and Technical Drawings

The assembly and disassembly of our machine was intended to be fast and easy. The parts must be cleaned between each extrusion tests in order to prevent any buildup of concrete or other residues and to ensure the testing parameters are the same to produce valid data. The greatest problem was that concrete sometimes infiltrated the cutouts for the O-rings and compromised the seal, resulting in some seepage that could affect the testing.

Beginning with the base, we mount the square plate directly to the UTS with a large bolt.

Four partially threaded rods are inserted into the holes in the corner of the base and bolted on tight. These will remain bolted to the base throughout testing and only need to be

removed to pack the machine up flat. Before we attached the central base to what is currently mounted on the machine, we first connect the support rods that will extend above to support the upper plate lid, as seen in Figure 2 (bottom-left). Again, these will not need to be removed from the central base unless being packed.

At this point we attach the two assemblies together by lining up the outer holes of the central base with the rods from the bottom base, and bolt these together. These nuts need only be finger-tight as the connection must be broken to clean the machine after each test. The actual support rods are partially threaded, so the base rests on the shoulder between the threaded and unthreaded sections.

Prior to testing, we put an O-ring into the circular cutout seen in Figure 3 (bottom-left), then place the cylinder chamber into the cutout as well. We then load the mixed concrete into

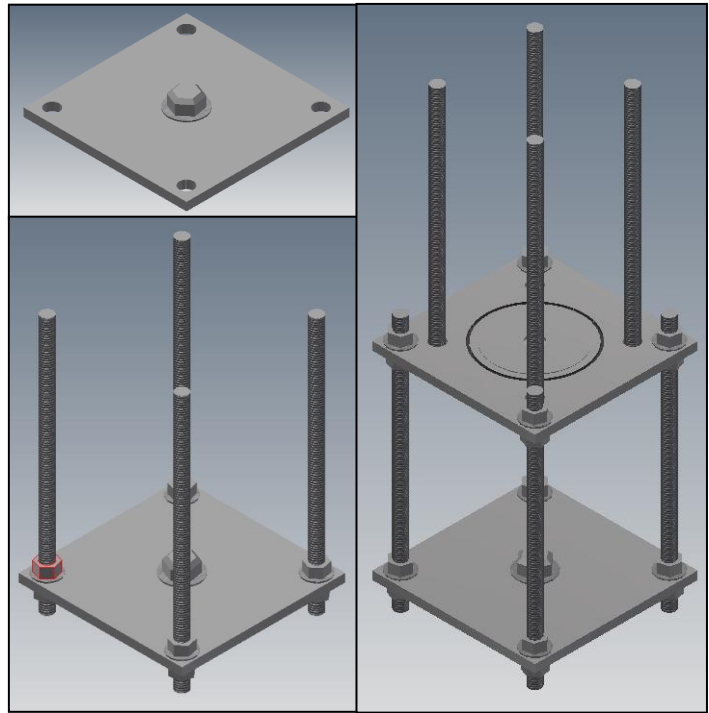


Figure 2. Various stages of assembly for the extruder apparatus.

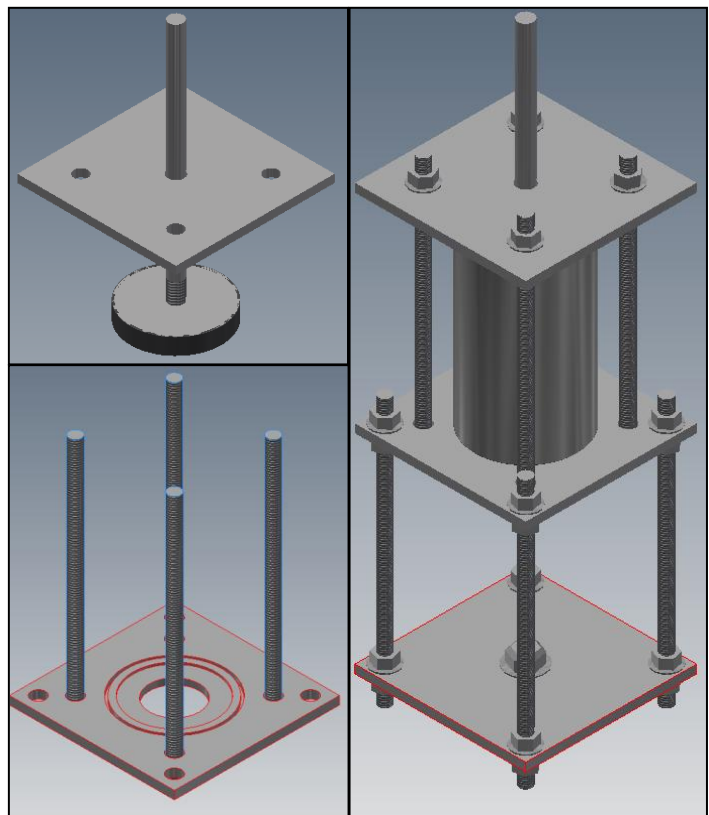


Figure 3. Various stages of assembly for the extruder apparatus.

the chamber, but must take care not to break the bottom seal before the machine is bolted tight, as concrete can get onto the O-ring and will prevent a strong seal later. We create one more sub-assembly of the upper lid and the plunger, which are attached together to ensure that the plunger is square with the cylinder and will line up with the UTS clamp that grips and pushes on it.

This is then carefully placed upon the mounted assembly once the concrete has been added. The upper plate also rests on the unthreaded shoulder of the rods, but the rods must be completely flush with the surface of the two plates that it is between. Because of a supplier error, the cylinder was slightly misshapen, as despite the efforts of our machinist to fix the mistake, it still did not sit quite right in the cutout it was meant to. We resorted to lightly tapping the plate with a hammer to get it flush, but ultimately we found a sweet spot where the cylinder fit perfectly into the cutouts and all four rods were perfectly mated between the plates, as seen in Figure 3 (right) with the entire assembly.

Fabrication Process

Again, the overall machine design is inspired by the work of Zhou and Li⁵ and adapted to fit the needs of this research and the UTM. Initial designs of the extrusion apparatus use threaded rods and nuts to create the spacers between the top and middle plate and between the bottom and the middle plate. The final design uses half-inch mild steel rod turned down to 3/8" and threaded on both ends to accommodate nuts. Each rod has a shoulder before the threads on which the plates sit. Each plate is made from type 304 stainless steel to avoid mechanical wear from the extruded paste and chemical corrosion from the cement. The bottom plate has a through hole in the middle to accommodate the bolt that secures the apparatus to the testing machine. The middle plate has a groove laid into its face to fit an O-ring and the bottom edge of the hopper. In the middle of the plate, there is a hole and a recessed face for interchangeable dies. These dies were turned down from 304 stainless steel rods. The fit between the middle plate and the nozzle is snug and there is no need for a gasket. The top plate has a through hole in the middle to help keep the piston arm from torqueing during testing. The cylinder purchased for the hopper came with an irregularity in shape that could not be corrected. In order to create a better seal, the ram has a groove on the side to fit an O-ring. Excessive frictional forces between the ram and the cylinder add noise to the collected data. Further designs of the machine need to include a more precise cylinder for the hopper. Apart from manufacturing flaws in the cylinder, the apparatus worked well overall.

Cost Analysis for Scale-up

Table 1. SINGLE-FAMILY PRICE AND COST BREAKDOWNS		
2009 National Results		
Average Lot Size:		21,879 sq ft
Average Finished Area:		2,716 sq ft
Sales Price Breakdown	Average	Share of Price
A. Finished Lot Cost (including financing cost)*	\$76,591	20.3%
B. Total Construction Cost	222,511	58.9
C. Financing Cost	6,375	1.7
D. Overhead and General Expenses	20,377	5.4
E. Marketing Cost	5,297	1.4
F. Sales Commission	12,815	3.4
G. Profit	33,658	8.9
Total Sales Price	\$377,624	100.0%
Construction Cost Breakdown	Average	Share of Constr. Cost
Building Permit Fees	\$4,264	1.9%
Impact Fee	3,165	1.4
Water and Sewer Inspection	3,761	1.7
Excavation, Foundation, and Backfill	15,878	7.1
Steel	1,637	0.7
Framing and Trusses	34,805	15.6
Sheathing	3,869	1.7
Windows	6,236	2.8
Exterior Doors	1,930	0.9
Interior Doors and Hardware	3,356	1.5
Stairs	1,676	0.8
Roof Shingles	8,472	3.8
Siding	12,858	5.8
Gutters and Downspouts	949	0.4
Plumbing	11,753	5.3
Electrical Wiring	8,309	3.7
Lighting Fixtures	2,372	1.1
HVAC	8,860	4.0
Insulation	3,332	1.5
Drywall	11,332	5.1
Painting	7,638	3.4
Cabinets and Countertops	12,444	5.6
Appliances	3,583	1.6
Tiles and Carpet	11,436	5.1
Trim Material	7,394	3.3
Landscaping and Sodding	7,088	3.2
Wood Deck or Patio	1,948	0.9
Asphalt Driveway	3,083	1.4
Other	19,085	8.6
Total	\$222,511	100.0%

Source: NAHB 2009 Construction Cost Survey, based on a national sample of 54 home builders

The printing process removes the need for framing, trusses, sheathing, insulation, and drywall – everything that goes into putting the skeleton of a traditional house together. This is a crucial step in the process, because for a home to be built well, all of the edges must be plumb and square with each other. Many traditional homes these days are built with the cheapest materials and labor that can be obtained, so one or the other is to blame when the floor is not quite level with the ceiling, or the house settles in a way that

causes significant damage. We not only eliminate the cost of labor for this part of construction, we ensure that the core of the house, upon which everything else is layered, is made exactly to specifications. There is much less room for human error to affect or slow the process, the way it does with traditional construction.

Additionally, while 3D printing the walls of the home, the printer is able to take a path that leaves vacancies in the structure for plumbing, electrical wiring, HVAC ducts, doors and windows, which would be installed once the main structure was built. This simplifies the task of installing these various systems, because the exact lengths, angles and locations will be given by the CAD model of the house from which the machine is deriving its paths. The necessary materials could be precut and labeled for its exact location, so workers need only put the pipes and wires in place and ensure all the connections and seals are strong. This speeds up the process substantially, and reduces material waste and scrap present in traditional construction.

The cost of the materials required for 3D printing houses would be much the same as that of a traditional house, in that it only replaces the materials used for constructing the walls and floors, while much of the materials for finishing the house and making it livable are the same. The advantage of 3D printing houses is that the process is sped up significantly by largely eliminating human labor (and reducing human error).

Life cycle analysis for concrete homes shows that they are also far more durable and resilient than traditional homes, and they are also much more energy efficient as well. In this, the 3D printed concrete home again beats out traditional methods, because it will cost less to heat and cool, and will last longer without needing any costly repair or upkeep.

An operation in China was able to print and assemble 10 houses in 24 hours, recycling industrial waste from previously demolished building for use in the 3D concrete printer. This largely reduces construction costs by eliminating the need for labor and accelerating the process, but the parts must be printed and then assembled, which introduces some human error in assembly.

Architects have also been working in Amsterdam to print a canal house using a 3D printer. Under their process, a single three-meter corner segment takes three weeks to be completed. The segments are printed from plastic and filled with concrete to give it more strength. The house is meant to take three years to complete, so this seems to be more of a novelty for the public and proof-of-concept of additive manufacturing in general than it is an actual construction method.

Finally, there is the Contour Crafting group at the University of South Carolina, who are working the implement 3D concrete printing to create low-income housing as well as emergency relief housing for war or natural disaster. Their method involves printing the concrete directly on the ground, rather than printing pieces and assembling them. This is much like how we envisioned the large-scale printing should be, to completely remove the human element from the initial construction process.

As we have stated, our goal was to create a system that would allow us to extrude and characterize new concrete formulations on a small scale in order to create accurate FLUENT simulations for modeling on a large scale. As such, new combinations of concrete, with different additives and aggregates, can be characterized and modeled rapidly to allow the novel mixture to be implemented on a larger scale.

Prototype Test Results

Our group started our testing process by using a control mixture that had sand making up 2% of the total volume. This deviated from what Zhou et al. did in their experiment, which was the background for our tests. Zhou used fibers for 2% of the total volume instead of sand. Our initial tests with sand gave force over time graphs that never plateaued. The force would constantly increase as if the concrete was being compressed, although extrusion was still taking place. This can be seen in Figure 4.

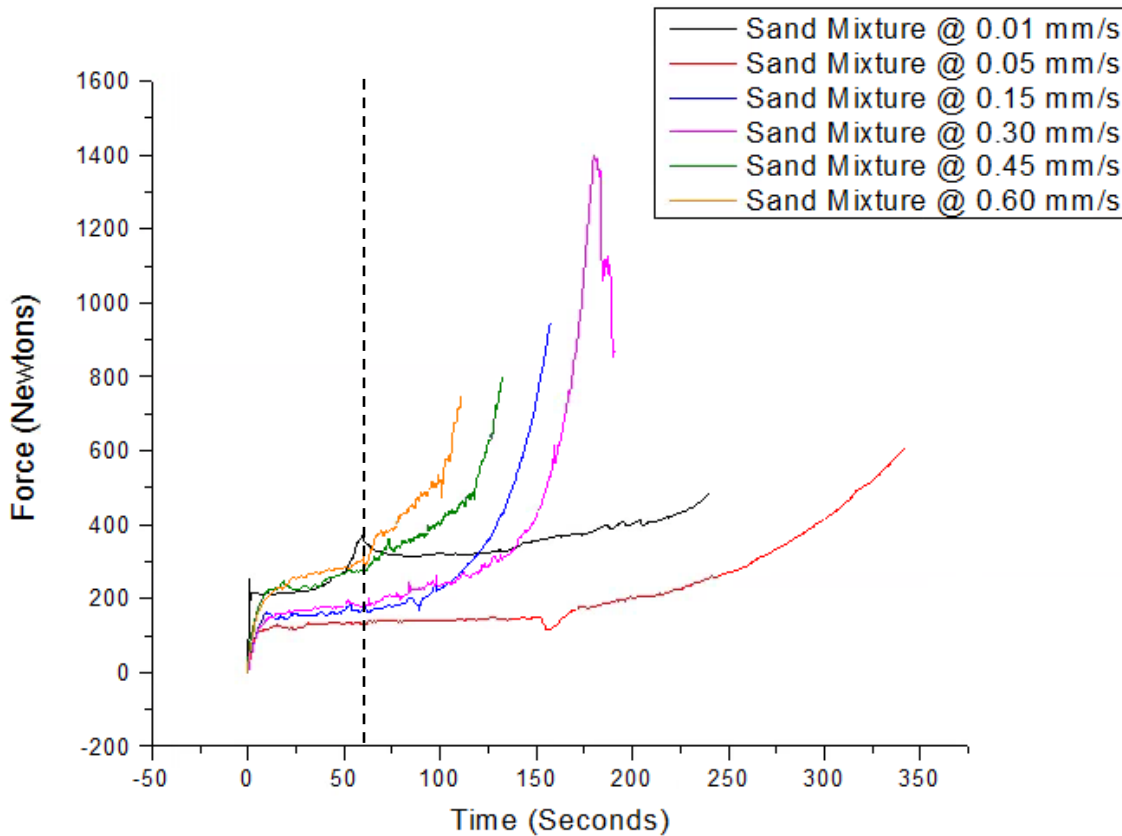


Figure 4. Required extrusion force of six samples of the sand and concrete mixture versus time. The dotted vertical line represents the change in extrusion speed from 0.01 mm/s to 0.01 mm/s (Dark Blue), 0.05 mm/s (Dark Red), 0.15 mm/s (Green), 0.35 mm/s (Purple) 0.45 mm/s (Blue) and 0.6 mm/s (Orange).

The data obtained for the concrete mixture with 2% total volume sand shows that as time increased, the concrete in the hopper became more and more dense. This negates the assumption that concrete is incompressible.

The control mixture that followed Zhou et al. by using 2% total volume polyvinyl alcohol (PVA) fibers gave data that was closer to Zhou et al.'s paper. The black line in Figure 5 represents the fiber control mixture. At first, the force is a constant lower value, which then increases linearly, peaks, and then plateaus. The plateau is difficult to see due to the large amount of noise in the data. However, this fiber control mixture was much more accurate to Zhou et al.'s mixture which is what we based our control on.

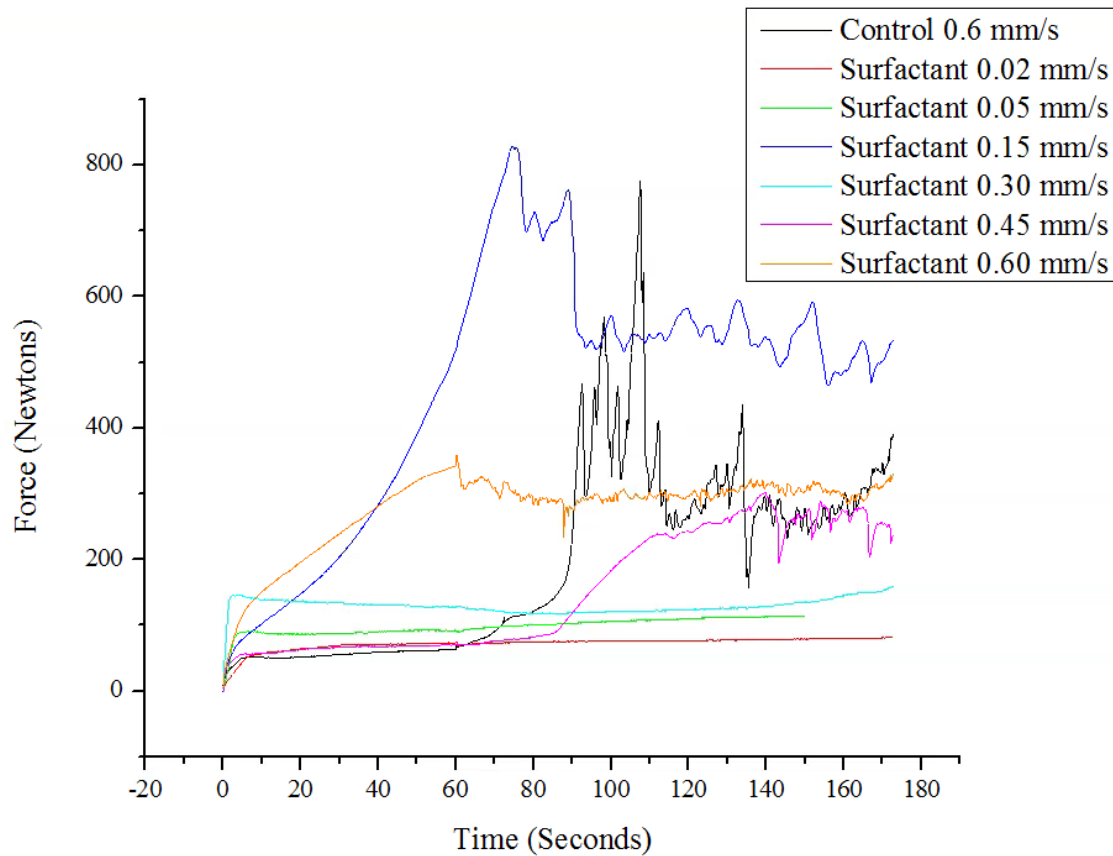


Figure 5. This graph shows Force versus Time for the control mixture and a mixture that had the control mixture as well as 0.30g of Air Entraining Surfactant. The surfactant mixtures were all mixed for two minutes.

The data for the surfactant mixtures, shown in Figure 5, all show very different force behaviors over time. All of the mixtures contained the same amount of admixtures, cement, silica fume and air entraining surfactant. The surfactant mixtures that were extruded at 0.15 mm/s, 0.45 mm/s and 0.6 mm/s all show curves that demonstrate a low applied force, linearly increasing applied force, and then a plateaued applied force. These curves show that the addition of surfactant did not significantly affect the force over time relationship that was established by the control mixture.

Another factor that affected our data was that all mixtures became properly hydrated at different water-to-binder ratios. This could possibly be due to initial mixing speeds or left over residue in the mixing container. The difference in consistencies between all mixtures is a large reason that the data we received could not be used in our FLUENT simulation. The test ran on our prototype did not give us enough data points to perform model fitting for the three Hershel-Bulkley parameters. The simulations that we performed used data gathered by Zhou et al.

When conducting this experiment, the duration of mixing was a variable that we changed. We expected to see that the longer that a mixture with surfactant is mixed, the more the mixture's workability would increase, and, thus, the less force would be required to extrude the mixture. We mixed two sets of batches, one set for 30 seconds and one set for three minutes. The two batches were identical in volume percent of all components including surfactant. However, water-to-binder ratios were different and this effect can be seen in Figure 6.

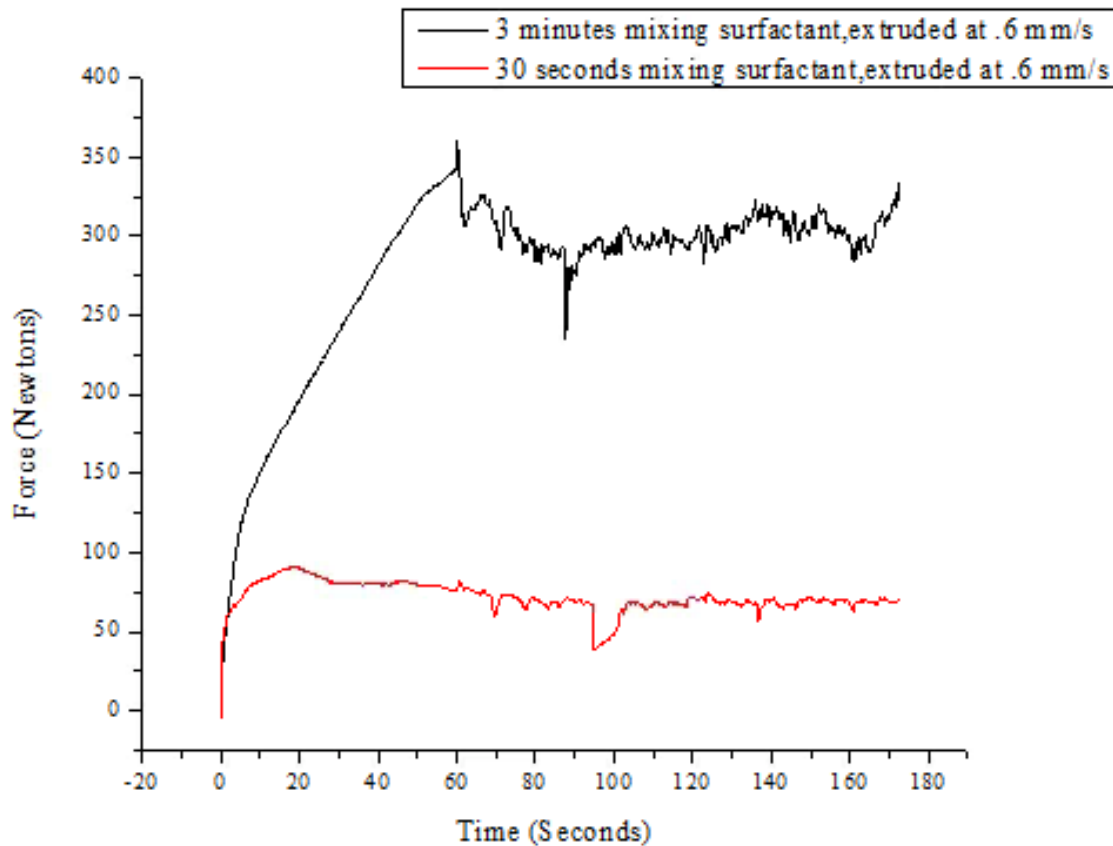


Figure 6. Force versus time for the same composition mixed for different lengths of time.

Mixing time played a factor on the amount of force required to extrude the air entrained mixtures. The surfactant mixture that was mixed for 30 seconds was extruded at a much lower applied force in comparison to the surfactant mixture that was mixed for three minutes. The differences in the curves could be due to the amount of time that the air entraining surfactant had to react with the cement mixture. The three-minute mixture had a much larger extrusion force, which could be due to the extended period of time that the air entraining surfactant had to react. Air entraining surfactant's purpose is to increase the workability of uncured cement, though, and our data does not demonstrate that. This could be because the water-to-binder ratio of the cement mixture in the 30-second mixture was off, and too much water was added. This would make the mixture less viscous, giving us the low extrusion force that is seen.

Assessment of Results

One of the most striking results is the difference in extrusion behavior between concrete with sand versus concrete with PVA fibers. We understand the fiber-reinforced concrete's behavior to be due to the yield stress of the concrete paste being met, and steady state flow occurring thereafter. This is demonstrated in the literature, and in fact is a requirement for fitting to the Herschel-Bulkey model from Zhou et al.⁵ With sand as the aggregate, we saw constantly increasing force, even while extrusion took place. We believe that this is because, under pressure, the cement was able to flow past the sand particles and exit the extruder, leading to an increasing concentration of sand particles within the hopper. This functioned to increase the remaining concrete's resistance to flow. The sand particles were untreated and possessed little chemical attraction to the aqueous cement paste. Additionally, the particles were roughly spherical in shape, reducing their ability to be carried along flow directions. The small diameter and high aspect ratio of the PVA fibers allowed them to flow out of the hopper with the cement.

The next result of interest is the nature and magnitude of the noise on our data plots (see Figure 5), as compared with our FLUENT simulation (see Figure 1). There are several possible sources of noise, including the particle nature of concrete, frictional rubbing of the ram on the hopper wall, and the release of entrapped air pockets during extrusion. An initial attempt at a Fourier transform of the noise during steady state extrusion is shown below in Figure 7, in an attempt to isolate the source of the noise. We believe that noise from frictional rubbing would display a preferred frequency, while noise from the particle nature of concrete (chaotic avalanches of particles) should not favor any frequency. The largest amplitudes of frequency occur at the minimum and maximum frequency, which could be interpreted as a preferred frequency from friction. We would not draw any conclusions, however, without further testing and analysis. It could be instructive to perform the same analysis on data using a hopper without the structural irregularities that ours possesses, to see if the same frequency peak exists even when there is no obvious source of frictional rubbing.

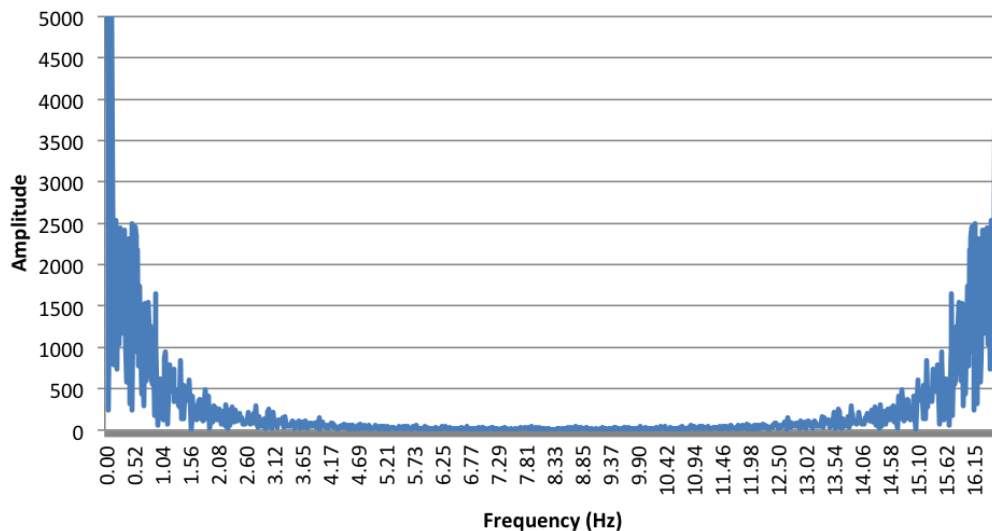
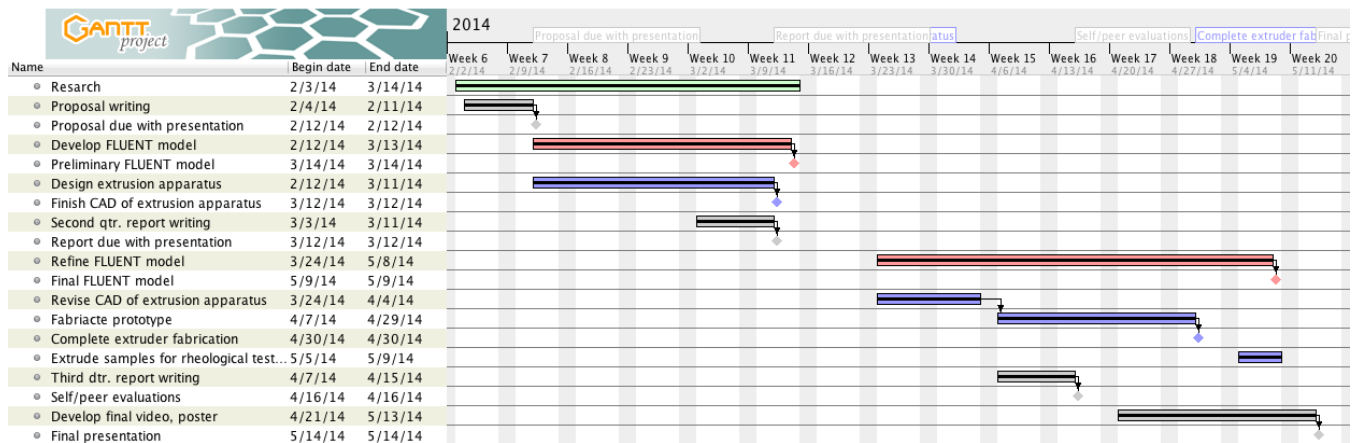


Figure 7. Fourier transform of noise during steady state extrusion.

Finally, our FLUENT simulation data shows general agreement with our experimental data, although without the noise discussed above. We believe that the Herschel-Bulkley model is a reasonable fit for fresh concrete pastes and that our data demonstrate a proof-of-concept for a CFD simulation of extrusion using a Herschel-Bulkley fluid. Additional work that could be done to better understand the limitations of the Herschel-Bulkley model is discussed in the Future Work section.

Timeline

Our final project timeline is shown below, although it has changed significantly over the course of the semester. The reasons for this are best described in the Project Selection Process and Evolution section. Of note is the extended time needed for the extruder apparatus to be designed and fabricated and the limited scope of testing as a result. We believe that with more time spent with a working prototype, we would gain deeper insights into the core issues of this investigation. Additionally, some processes, such as curing, take up to 28 days to meet industry specifications, and such a time span was hardly feasible in this project. However, future work could certainly involve studying both the fresh and hardened properties of extruded concrete to better understand some of the phenomena at work.



Budget

Below is our completed budget. The bulk of our budget was spent on the extruder apparatus. Luckily, many of the concrete constituents and admixtures were available for free through suppliers due to our academic status. We had not planned to work so close to the top of our budget, but our machinist increased his pricing unexpectedly in order to cover materials and tools that he purchased or used in order to machine the extruder, although these costs were not included in his initial quote.

CATEGORY	ITEM	UNIT COST	TOTAL COST
FACILITIES	MEMIL lab usage	—	—
APPARATUS	Hopper	—	\$73
	Piston	—	\$80
	Plates	\$24	\$72
	Extruder dies	\$10	\$30
	Connection hardware	—	\$50
	Machinist labor	—	\$500
CONCRETE	Portland cement	—	—
	Sand	—	—
	Water	—	—
	Surfactant, 8 oz.	—	—
	Fibers, 1 lb.	—	—
	Superplasticizer, 2.5 lb.	—	\$17
	Silica fume, 10 oz.	—	—
	Fly ash	—	—
	Retarder	\$3	\$9
MISC.	Mixing paddle	—	\$12
	Drop cloth	—	\$11
PRESENTATION	Poster	—	\$70
SHIPPING	Total shipping costs	—	\$73
		TOTAL	\$997

Future Work

There are several interesting phenomena that merit future investigation. We know that the choice of aggregate can alter the fresh properties of concrete, but future studies could determine the effects of average aggregate diameter, distribution, and composition on concrete extrudability. This could include using sand that has been surface treated to avoid desegregation, or fibers of varying aspect ratios. While we introduced an air entraining admixture with two levels of mixing time, inconsistencies between batches obscured the relationship between entrained air bubble size and extrudability. An entire investigation could be made in understanding the effectiveness of air entrainers in thick concrete pastes with low water content. To model the discrete particle phases, we could transfer our model into ANSYS POLYFLOW, which allows for the simultaneous modeling of Herschel-Bulkley fluids and discrete phases. Some other important considerations are more accurate material property measurements, wall-interface behavior, and modeling for air bubble-air bubble interactions. We believe that with more time, though, a custom simulation tool should be developed that does not depend on a commercial product where it is unclear what assumptions are being made. Finally, any simulation tool should undergo experimental validation against a variety of concrete compositions and extrusion conditions.

REFERENCES

1. National Academy of Engineering. Restore and improve urban infrastructure - Engineering Challenges. (2014). at <<http://www.engineeringchallenges.org/cms/8996/9136.aspx>>
2. Le, T. T. *et al.* Mix design and fresh properties for high-performance printing concrete. *Mater. Struct.* **45**, 1221–1232 (2012).
3. Le, T. T. *et al.* Hardened properties of high-performance printing concrete. *Cem. Concr. Res.* **42**, 558–566 (2012).
4. Lim, S. *et al.* Developments in construction-scale additive manufacturing processes. *Autom. Constr.* **21**, 262–268 (2012).
5. Zhou, X., Li, Z., Fan, M. & Chen, H. Rheology of semi-solid fresh cement pastes and mortars in orifice extrusion. *Cem. Concr. Compos.* **37**, 304–311 (2013).
6. Khoshnevis, B. Automated construction by contour crafting—related robotics and information technologies. *Autom. Constr.* **13**, 5–19 (2004).
7. *Simulation of Fresh Concrete Flow: State-of-the Art Report of the RILEM Technical Committee 222-SCF.* 147 (Springer, 2014).
8. Zhou, X. & Li, Z. Numerical simulation of ram extrusion in short-fiber-reinforced fresh cementitious composites. *J. Mech.* **4**, 1755–1770 (2009).